

# Lepton-Jets and Low-Mass Sterile Neutrinos at Hadron Colliders

Sourabh Dube,<sup>1,\*</sup> Divya Gadkari,<sup>1,2,†</sup> and Arun M. Thalapillil<sup>1,‡</sup>

<sup>1</sup>*Indian Institute of Science Education and Research,  
Homi Bhabha road, Pashan, Pune 411008, India.*

<sup>2</sup>*Department of Physics, LEPP, Cornell University, Ithaca, NY 14853, USA.*

(Dated: October 18, 2024)

Sterile neutrinos, if they exist, are potential harbingers for physics beyond the Standard Model. They have the capacity to shed light on our flavor sector, grand unification frameworks, dark matter sector and origins of baryon anti-baryon asymmetry. There have been a few seminal studies that have broached the subject of sterile neutrinos with low, electroweak-scale masses (i.e.  $\Lambda_{\text{QCD}} \ll m_{N_R} \ll m_{W\pm}$ ) and investigated their reach at hadron colliders using lepton jets. These preliminary studies nevertheless assume background-free scenarios after certain selection criteria which are overly optimistic and untenable in realistic situations. These lead to incorrect projections. The unique signal topology and challenging hadronic environment also make this mass-scale regime ripe for a careful investigation. With the above motivations, we attempt to perform the first systematic study of low, electroweak-scale, right-handed neutrinos at hadron colliders, in this unique signal topology. There are currently no active searches at hadron colliders for sterile neutrino states in this mass range, and we frame the study in the context of the 13 TeV high-luminosity Large Hadron Collider and the proposed FCC-hh/SppC 100 TeV  $pp$ -collider.

## I. INTRODUCTION

With the discovery of the Higgs-boson-like resonance at the LHC [1, 2], we are very quickly approaching a detailed understanding of electroweak symmetry breaking and mass generation in the SM. The presence of fermion mass hierarchies (i.e. hierarchies among the Yukawa coupling constants) nevertheless remain a mystery. The Yukawa couplings that span across many orders of magnitude and the appearance of mass ratios that are seemingly very close to powers of the Cabibbo angle (see for instance [3] and references therein) along with patterns in the quark and lepton mixing matrices seem to suggest that the flavor sector of the SM may have a rich underlying structure.

All the current experiments are largely consistent with the existence of three neutrino electroweak eigenstates ( $\nu_e, \nu_\mu, \nu_\tau$ ). Nevertheless, there have been a few tantalising discrepancies from various short-baseline neutrino experiments [4–7] over the years. They have occasionally been very hard to accommodate in the three active-neutrino picture, leading to many studies incorporating additional singlet neutrino states to the framework [8–22]. For instance, trying to accommodate the LSND [4] and MiniBooNE [5] anomalies

with observations from solar and atmospheric neutrino measurements require  $\Delta m_{\text{sterile}}^2 \sim \mathcal{O}(1) \text{eV}^2$ . A similar mass squared difference is also seemingly required to reconcile the reactor anti-neutrino flux deficit [7], but this interpretation has been weakened recently [23]. On the other hand, embedding frameworks leading naturally to light neutrino masses, such as the see-saw mechanism [24], into grand unified models [25–33] furnishes singlet neutrino states that are extremely heavy with a mass  $\mathcal{O}(10^{12} - 10^{16}) \text{GeV}$ . These have the added benefit of mitigating, to some extent, fine-tuning of the neutrino Yukawa coupling constants. In these models Yukawa couplings may be  $\mathcal{O}(1)$  and the large hierarchy in mass is subsequently generated, after mass diagonalization. There are also intriguing models [34–37] with sterile neutrino states below the  $\Lambda_{\text{QCD}}$  scale with masses  $\mathcal{O}(1) \text{keV}$  that may simultaneously be able to explain structures in the lepton sector, provide dark-matter candidates as well as furnish a solution to the baryon anti-baryon asymmetry observed in the universe. Along with these considerations perhaps there is also another aspect to be kept in mind – a small right-handed neutrino mass ( $m_{\nu_R}^M$ ) must be considered technically natural, as emphasised by [38, 39], since in the limit  $m_{\nu_R}^M \rightarrow 0$  one regains  $U(1)_{\text{B-L}}$  as a global symmetry of the Lagrangian.

The above considerations suggest that *a priori* there are perhaps no immutable reasons to expect the right-handed neutrino mass-scale to be at a particular value. Motivated by this realization it is reasonable to devise

\* [sdube@iiserpune.ac.in](mailto:sdube@iiserpune.ac.in)

† [divya.gadkari@students.iiserpune.ac.in](mailto:divya.gadkari@students.iiserpune.ac.in)

‡ [thalapillil@iiserpune.ac.in](mailto:thalapillil@iiserpune.ac.in)

search strategies for sterile neutrinos that cover all possible mass-scales.

There has indeed been endeavours to directly and indirectly search for sterile neutrino states across various mass scales (see for instance [40–44] and references therein). For instance, in [45] the sensitivity of a future lepton collider to displaced vertex searches were investigated in final states  $e^+e^- \rightarrow \nu(N \rightarrow l^\pm jj, l^+l^-\nu, \dots)$ . A similar, earlier study [46] based on displaced vertices at the LHC investigated processes such as  $pp \rightarrow l^\pm(N \rightarrow l^\pm X)$ . Another study in [47] advocated looking for processes  $W^+ \rightarrow e^+\mu^-e^+\nu_e$  and  $W^+ \rightarrow e^+e^+\mu^-\bar{\nu}_\mu$  initiated by sterile neutrinos at the LHC; the latter being initiated only in the case of Majorana sterile neutrinos. Studies such as [48] focused on left-right symmetric models with a heavy  $W_R$ , leading to ‘neutrino-jet’ final states  $W_R \rightarrow l(N \rightarrow ljj)$ ; where the  $N$  decay-products are collimated even for  $m_N \gg m_{W^\pm}$ . Recently, there have also been interesting studies attempting to constrain electroweak-scale sterile neutrinos through precision Higgs data [49] and Higgs decays [50]. A more complete discussion of current theoretical studies and limits, across various mass-scales, is contained in [40–44] and associated references.

The ATLAS and CMS collaborations have performed dedicated searches for heavy Majorana neutrinos [51–54] in various channels. The CMS collaboration has looked for heavy sterile neutrinos in  $\mu^\pm\mu^\pm jj$ ,  $e^\pm e^\pm jj$  and  $e^\pm\mu^\pm jj$  final states at  $\sqrt{s} = 8$  TeV with  $19.7 \text{ fb}^{-1}$  of data [51, 52]. The ATLAS collaboration has similarly searched for heavy Majorana neutrinos in the  $\mu^\pm\mu^\pm jj$  and  $e^\pm e^\pm jj$  channels at  $\sqrt{s} = 8$  TeV using  $20.3 \text{ fb}^{-1}$  of collected data [53]. The CMS collaboration has also recently set preliminary limits at  $\sqrt{s} = 13$  TeV [54], with  $2.3 \text{ fb}^{-1}$  data, for heavy composite Majorana neutrinos in final states with two leptons and two quarks. All the current LHC constraints for the  $l^\pm l^\pm jj$  channels are summarised in Fig. 1.

We are interested in probing a regime where the sterile neutrino states have a mass above the bottom-quark mass ( $m_b$ ) but is at the same time well below  $m_{W^\pm}$

$$\Lambda_{\text{QCD}} \ll m_b < m_{N_R} \ll m_{W^\pm} .$$

In this narrow mass-region, the existing constraints are minimal and the signal topology is unique while being challenging. We shall sharpen and motivate the region of interest in more detail in Sec. III. The prototypical signal event is illustrated in Fig. 2. In this region the sterile neutrino is usually very boosted and the decay products get collimated into a lepton jet.

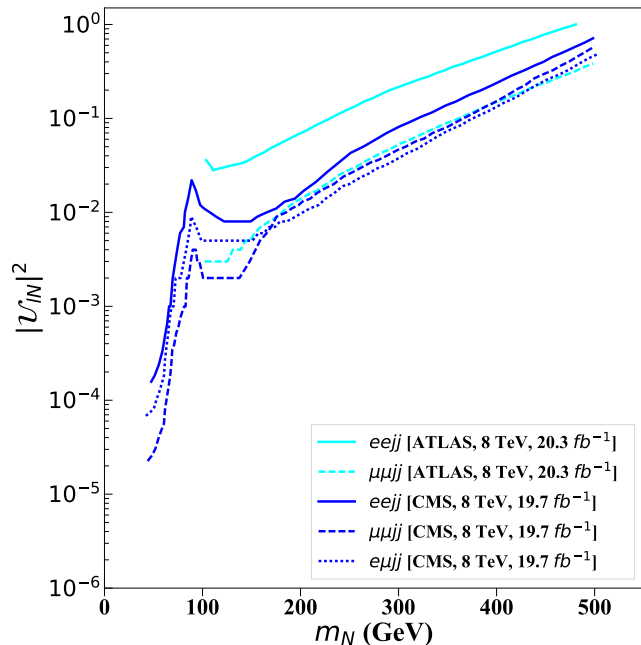


FIG. 1. Current constraints on sterile-active mixing ( $|U_{lN}|$ ) from the ATLAS and CMS collaborations [51–53]. The relevant final states being searched for are like-sign leptons with associated jets ( $l^\pm l^\pm jj$ ) in all the present analyses. Few of the CMS limits go all the way to intermediate masses of around 50 GeV. The preliminary limit from CMS for  $\sqrt{s} = 13$  TeV with  $2.3 \text{ fb}^{-1}$  of data [54] is not shown.

$$pp \rightarrow l^\pm + (N_R \rightarrow \text{Lepton Jet}) + X \quad (1)$$

There have been a few hadron collider studies specifically focused on this region [44, 55]. The pioneering study [55] assumed a background-free search, employing certain selection criteria, with cosmic-ray initiated muon bundles estimated based on an ATLAS analysis [58]; the latter looked for long-lived neutral particles in LHC events with two lepton jets. Based on these estimates, limits at 13 TeV LHC are set in this region, assuming an integrated luminosity of  $300 \text{ fb}^{-1}$ . Similarly, the study pertaining to this mass-scale discussed in [44] for  $pp$ -colliders, assumes that there are no backgrounds for  $1 \text{ mm} < c\tau < 1 \text{ m}$  vertex displacements. With this and a few other assumptions, the study estimates preliminary limits for the high-luminosity LHC (HL-LHC) at 13 TeV and the FCC-hh/SppC  $pp$ -collider at 100 TeV [56, 57]. They conclude by acknowledging that a realistic estimate of the backgrounds and sensitivities is very much required in

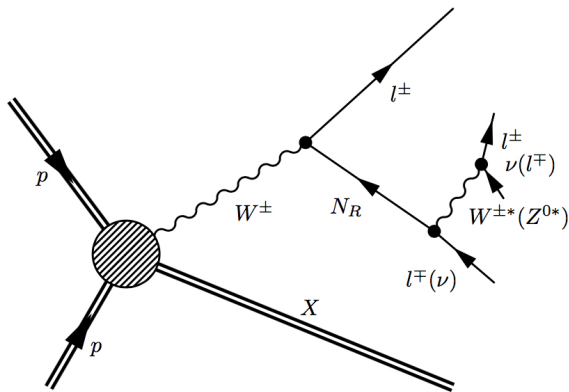


FIG. 2. In the mass regime of interest,  $m_b < m_{N_R} \ll m_{W^\pm}$ , the main production channel at hadron colliders is through single- $W^\pm$  production and decay. Since  $m_{N_R}/m_{W^\pm} \ll 1$  the leptons from the  $N_R$  decay are collimated and form a displaced lepton jet in the relevant parameter space [55]. The lepton from the initial  $W^\pm$  decay is detected as a prompt lepton.

this mass-regime.

As we shall discuss in Secs. III and IV, the above search methodologies, selection criteria and considerations regarding signal and backgrounds have to be drastically modified under realistic conditions. Our aim is to perform a systematic study in this mass-scale regime and investigate realistic selection criteria that optimise searches for these light sterile neutrinos at hadron colliders. Towards this aim we explore the discovery potential at the 13 TeV LHC and the proposed FCC-hh/SppC 100 TeV  $pp$ -collider [56, 57]. In this low mass-scale regime the decay products from the right-handed neutrino get collimated into a narrow cone [55]. As we elaborate in Secs. III and IV, we will therefore optimise for a topology consisting of a prompt lepton and a collimated set of muons, a muon lepton-jet.

One of the main constraints in the region of interest comes from electroweak precision data [59–63]. To very good approximation, the limits on active-sterile mixing ( $|\mathcal{U}_{lN}|^2$ ), from electroweak precision data, are found to be almost independent of the sterile neutrino masses in this region. At 90% confidence level they are approximately given by  $|\mathcal{U}_{eN}|^2 \leq 3 \times 10^{-4}$ ,  $|\mathcal{U}_{\mu N}|^2 \leq 1.5 \times 10^{-4}$  and  $|\mathcal{U}_{\tau N}|^2 \leq 13 \times 10^{-4}$  [42, 59–63].

The other major constraint in this mass regime comes from limits on heavy sterile states produced in  $Z^0$  decays. The L3 [64] and DELPHI [65] collaborations have performed a reanalysis of the LEP data

in this context. The former sets a limit  $|\mathcal{U}_{lN}|^2 \lesssim (0.7 - 1.0) \times 10^{-4}$ , corresponding to a limit on the branching ratio  $\text{Br}(Z^0 \rightarrow \bar{\nu}N) \lesssim 10^{-5}$  [66], in the region of interest. The DELPHI analysis puts a limit  $\text{Br}(Z^0 \rightarrow \bar{\nu}N) \lesssim 1.3 \times 10^{-6}$  at 95% C.L. which corresponded to  $|\mathcal{U}_{lN}|^2 \lesssim 10^{-5}$  [65].

In Sec. II, to clarify notations and put our study in context, we briefly discuss the well known theoretical motivations for sterile neutrinos. Here, we also briefly consider models where low-mass right-handed neutrinos could arise in a natural way. In Sec. III we then discuss the unique signal topology furnished by sterile neutrinos in the mass regime of interest and also discuss aspects of the various relevant backgrounds. Then, in Sec. IV we present our analysis methodologies and main results. We summarise our pertinent findings in Sec. V.

## II. RIGHT-HANDED STERILE NEUTRINOS AND THE STANDARD MODEL

The inexplicable and large hierarchies among the fermion masses manifests in its most extreme form in the case of neutrinos. To clarify notations and set context we briefly consider the theoretical underpinnings behind sterile neutrinos and specific models where low, electroweak-scale masses could be generated for these states.

Neutrino oscillation experiments only furnish information about mass-squared differences [67]. Through careful endpoint measurements of the tritium  $\beta$ -decay spectrum, Troitzk [68] and Mainz [69] experiments were able to put an upper limit at 95% C.L. of about

$$m_\nu < 2 \text{ eV} . \quad (2)$$

Light neutrinos play a significant role in cosmology, by effecting the expansion history and the growth of primordial structures, which in combination with other astrophysical and cosmological observations, lead to an even tighter bound [70–72]

$$\sum m_\nu < 0.23 \text{ eV} .$$

The KATRIN experiment [73] is expected to reach a sensitivity close to  $m_\nu < 0.2 \text{ eV}$  as well.

All these observations suggest that the neutrinos in the SM have a mass-scale in the sub-eV regime. The neutrinos with SM quantum numbers thus seem to have a mass-scale at least a million times smaller than the next heaviest fermion, the electron. If not an accident of nature, these small neutrino masses beg for an explanation.

In the standard model, the neutrinos have just a single left-helicity field associated with them and therefore one cannot directly write a Dirac mass term in the usual way. One could of course extend the framework minimally by adding just a right-handed helicity neutrino field, thereby giving neutrinos a Dirac mass after electroweak symmetry breaking<sup>1</sup>

$$\mathcal{L}_{\text{mass}} \supset m_\nu^D (\bar{\nu}_L \nu_R + \bar{\nu}_R \nu_L) \equiv m_\nu^D \bar{\nu} \nu . \quad (3)$$

If this was the only contribution, the relevant yukawa coupling here has to be fine-tuned to a very small value, to be consistent with the sub-eV mass-scale of the neutrinos. The interesting observation is that, since the right-handed neutrino field carries no SM charges, one is allowed to also write an additional contribution to the mass of the form

$$\mathcal{L}_{\text{mass}} \supset m_{\nu_R}^M (\bar{\nu}_R^c \nu_R + \bar{\nu}_R \nu_R^c) \equiv m_{\nu_R}^M \bar{\chi} \chi , \quad (4)$$

i.e. a Majorana mass term. Here, the charge conjugation is defined as  $\psi^c = i\gamma^2 \psi^*$ , with the notation  $\psi_R^c = (\psi_R)^c$  and the Majorana field  $\chi$  is defined to be  $\chi = \nu_R + \nu_R^c$ . Note that a similar term with  $\nu_L$  would be forbidden in this minimal scheme due to SM gauge invariance – the  $\nu_L$  field is part of the  $SU(2)_L$  doublet with non-zero hypercharge.

This additional contribution enables a novel way in which the very-small neutrino masses could be generated – the so called see-saw mechanism [24]. As motivated above, in its simplest form it leads to a neutrino mass-matrix of the form

$$\mathcal{M}_\nu = \begin{pmatrix} 0 & \frac{1}{2} m_\nu^D \\ \frac{1}{2} m_\nu^D \text{ }^\top & m_{\nu_R}^M \end{pmatrix} . \quad (5)$$

Taking for example the simplest 1-flavor case, with a  $2 \times 2$  mass-matrix, leads to mass-eigenvalues

$$m_{1,2} = \frac{1}{2} \left[ m_{\nu_R}^M \pm \sqrt{m_{\nu_R}^{M2} + m_\nu^{D2}} \right] , \quad (6)$$

with two Majorana eigenstates

$$\begin{aligned} \nu_1 &= \tilde{\chi} \cos \theta - \chi \sin \theta \\ \nu_2 &= \tilde{\chi} \sin \theta + \chi \cos \theta . \end{aligned} \quad (7)$$

Here,  $\chi = \nu_R + \nu_R^c$  as before,  $\tilde{\chi} = \nu_L + \nu_L^c$  and the mixing angle is defined as

$$\tan 2\theta = - \frac{m_\nu^D}{m_{\nu_R}^M} . \quad (8)$$

If one assumes that  $m_{\nu_R}^M \gg m_\nu^D$ , then one obtains a light and heavy neutrino state, as is well known,

$$\nu_l \sim \tilde{\chi} , \quad \nu_h \sim \chi , \quad (9)$$

with masses

$$m_l \sim - \frac{m_\nu^{D2}}{m_{\nu_R}^M} , \quad m_h \sim m_{\nu_R}^M . \quad (10)$$

Observe that the heavier state is a right-handed majorana fermion.

Note also from the above discussions that the mixing matrix elements  $|\mathcal{U}_{lN}|$ , between active and right-handed (sterile) states, roughly scale like  $m_\nu^D m_{\nu_R}^{M-1}$ . If one had  $m_\nu^D \sim \mathcal{O}(\text{EW-scale})$ , hence seemingly mitigating to some extent the relative hierarchy among Yukawa couplings, then this would imply  $m_{\nu_R}^M \sim \mathcal{O}(10^{12} - 10^{15} \text{ GeV})$  to get viable light neutrino masses in this simplest framework. This right-handed Majorana scale is also attractive from the point of view grand unified theories [74], specifically left-right symmetric grand unified models such as the Pati-Salam model [75]. The above discussions may be extended to the case of two or more sterile neutrinos. The inclusion of additional sterile neutrinos to the three active ones adds more structure to the neutrino sector.

On the other hand, as we alluded to before, it must be noted that low  $m_{\nu_R}^M$  scales must be considered technically natural [38, 39] – since in the limit  $m_{\nu_R}^M \rightarrow 0$  one regains  $U(1)_{B-L}$  as a global symmetry of the Lagrangian. In this context, the presence of additional states in a k-neutrino framework furnishes new possibilities. One could now have novel flavor structures, under seesaw or non-seesaw scenarios, sometimes augmented by lepton-number-like family symmetries. In many of these models the right-handed neutrino mass-scale is unconstrained and could in general be small, leading to interesting observational consequences [38, 39, 76–87].

All of these thus imply, as we mentioned earlier, that *a priori* it is prudent to be agnostic about the exact  $m_{\nu_R}^M$  scale and devise search strategies that would span the full range of possibilities. We will be specifically interested in scenarios where  $m_{\nu_R}^M \ll m_{W^\pm}$ , i.e. in the low, electroweak-scale regime. In these scenarios the mixing between the active-sterile states could be larger than naive expectations and potentially unsuppressed. For instance, in inverse seesaw models [77, 78] – the simplest realization of which has three extra standard model singlet neutral fermions ( $\Psi$ ) in addition to three generations of sterile ( $N_R$ ) and active neutrinos ( $\nu_L$ )–

<sup>1</sup> Flavor indices are suppressed in the following discussions for clarity.

the Lagrangian takes the form

$$\mathcal{L}_{\text{mass}}^{\text{inv. see-saw}} \supset -M_D \bar{\nu}_L N_R - M \bar{\Psi}_L N_R - \frac{\delta}{2} \bar{\Psi}_L \Psi_L^c, \quad (11)$$

which leads to a neutrino mass-matrix

$$\mathcal{M}_\nu = \begin{pmatrix} 0 & M_D & 0 \\ M_D^T & 0 & M \\ 0 & M^T & \delta \end{pmatrix}. \quad (12)$$

Note that as  $\delta \rightarrow 0$  one regains the lepton-number-like protection symmetry, and hence a small  $\delta$  is technically natural.

On diagonalizing the mass matrix, assuming a hierarchy among the scales  $\delta \ll M_D \lesssim M$ , the mass of the light neutrinos scale as

$$m_\nu \sim \delta \frac{M_D^2}{M^2}, \quad (13)$$

while the active-sterile mixing matrix elements still scale as

$$|\mathcal{U}_{lN}| \sim \frac{M_D}{M}. \quad (14)$$

Owing to the presumably small  $\delta$  and the difference in scaling behavior between masses and mixing angles, we have the possibility of getting very small SM neutrino masses, while retaining the possibility of relatively light sterile neutrinos. The latter could also have significant mixing with active neutrinos ( $|\mathcal{U}_{lN}| \sim M_D/M \lesssim \mathcal{O}(1)$ ). This could lead to effective couplings between the sterile states and the  $W^\pm$ ,  $Z^0$  vector gauge bosons that are relatively unsuppressed. Thus, the relatively large mixing angles along with the lighter masses open the way for these right-handed sterile states to be searched for in particle collider experiments.

In the mass-range we are interested in,  $m_b < m_{N_R} \ll m_{W^\pm}$ , the dominant production mode for a sterile neutrino are through  $W^\pm$  charged-current and  $Z^0$  neutral-current interactions, mediated through the mixings with active-neutrino states,

$$\begin{aligned} pp &\rightarrow W^\pm + X \rightarrow l^\pm N_R + X, \\ &\hookrightarrow Z^0 + X \rightarrow \nu N_R + X. \end{aligned}$$

For higher  $m_{N_R}$ , production may also occur competitively through collinear enhanced processes with t-channel photon exchange, such as  $pp \rightarrow W^{\pm*} \gamma^* jj \rightarrow N l^\pm jj$  [88]. For masses below the bottom-quark mass,  $m_{N_R} < m_b$ , production through  $B$ -meson decay channels also open up.

The right-handed neutrinos after being produced subsequently decay, again through  $W^\pm$  charged-current or  $Z^0$  neutral-current interactions mediated by active-sterile mixing. The partial widths to leptonic final states are given by [41, 89]

$$\begin{aligned} \Gamma(N_R \xrightarrow{W^*} l_a^- l_b^+ \nu_b) &= \frac{G_F^2}{192\pi^3} m_N^5 |\mathcal{U}_{aN}|^2, \\ \Gamma(N_R \xrightarrow{W^*/Z^*} l_a^- l_a^+ \nu_a) &= \frac{G_F^2}{96\pi^3} m_N^5 |\mathcal{U}_{aN}|^2, \\ &\quad (\hat{g}_L^2 + \hat{g}_L \hat{g}_R + \hat{g}_R^2 + 2\hat{g}_L + 2\hat{g}_R + 1), \\ \Gamma(N_R \xrightarrow{Z^*} \nu_a l_b^+ l_b^-) &= \frac{G_F^2}{96\pi^3} m_N^5 |\mathcal{U}_{aN}|^2 (\hat{g}_L^2 + \hat{g}_L \hat{g}_R + \hat{g}_R^2), \\ \Gamma(N_R \xrightarrow{Z^*} \nu_a \nu_b \bar{\nu}_b) &= \frac{G_F^2}{768\pi^3} m_N^5 |\mathcal{U}_{aN}|^2. \end{aligned} \quad (15)$$

Here the SM couplings are defined as  $\hat{g}_L = \frac{1}{2} + \sin^2 \theta_w$  and  $\hat{g}_R = \sin^2 \theta_w$ .

We are interested in devising an optimal search strategy for low, electroweak-scale sterile neutrinos produced at  $pp$ -colliders; dominantly via decays of  $W^\pm$  and which decay through their charge-current interactions. The typical process of interest is therefore

$$pp \rightarrow W^\pm + X \rightarrow l_a^\pm (N_R \rightarrow l_a^\mp \nu_a) + X, \quad (16)$$

as shown in Fig. 2.

In the next section we will take a closer look at the event and background topologies to be expected and discuss considerations that must be taken into account for an effective search at the LHC and the proposed 100 TeV  $pp$ -colliders.

### III. EVENT TOPOLOGY AND BACKGROUNDS

Traditional multilepton searches (for example Ref. [90, 91]) can have high sensitivity for sterile neutrinos with masses above  $\sim 100$  GeV. These searches rely on prompt, well-separated (and isolated) leptons in the final state, and typically require lepton transverse momenta ( $p_T$ ) to satisfy  $p_T > 20$  GeV. With careful selection of isolation criteria, and lowering of the lepton  $p_T$  threshold, or by considering final states with dileptons and jets, the sensitivity can be extended to sterile neutrino masses as low as 50 GeV [51, 52].

However as the mass of the sterile neutrino becomes lighter, which is the case of interest in our current investigation, new search strategies need to be explored. One such interesting final state involves a prompt lepton along with a lepton-jet [55]. In a lepton-jet, two



or more leptons lie very close to each other in the detector. Such a signature will be rejected by standard isolation criteria, and needs a separate, special selection criteria. Lepton-jet searches have been carried out by the LHC experiments in the context of different new physics models. ATLAS searches for pairs of lepton-jets [92] which might or might not be significantly displaced from the interaction point. CMS searches for a pair of leptons [93] which may lie close to each other, but which are displaced and need to satisfy  $m_{\ell\ell} > 15$  GeV. The CMS search also has stiff requirements on lepton  $p_T$ .

A different approach is needed to probe for sterile neutrinos that lie in the range  $m_b < m_{N_R} \ll m_{W^\pm}$ . We choose a final state that consists of a lepton-jet accompanied by the presence of a prompt, well-isolated lepton. This choice of final state dictates the analysis strategy, since it significantly affects which standard model processes will act as a background to the search. Further selections to optimize the sensitivity are then governed by the interplay between the signal of interest, the backgrounds and the specific selections.

The particular decay chain we probe is  $W^\pm \rightarrow \ell^\pm N_R \rightarrow \ell^\pm \ell'^\pm \ell''^\mp \nu$ . Here the  $\ell$  arises promptly from the decay of the  $W^\pm$ , and has relatively high  $p_T$ . On the other hand, the  $\ell'$  and  $\ell''$ , which arise from the decay of the sterile neutrino ( $N_R$ ), are not necessarily prompt and can have low  $p_T$ , depending on the mass and lifetime of the  $N_R$ . Moreover, depending on the boost of the  $N_R$ , the  $\ell'$  and  $\ell''$  can also come close to each other forming a lepton-jet. Let us now consider each aspect of this signal topology carefully.

The separation between the decay products of  $N$  scale as  $\Delta R \sim m_{N_R}/p_T^{N_R}$  while in the rest frame of the  $W^\pm$  the momentum of the sterile neutrino scales as  $p_T^{N_R} \sim (m_{W^\pm}^2 - m_{N_R}^2)/m_{W^\pm}$ . This implies that around  $m_{N_R} \sim 20$  GeV the opening angle for the decay products will exceed  $\Delta R \sim 0.5$ . At around this mass the lepton-jet selection criteria will therefore become less efficient and one expects that the limits obtained near  $m_{N_R} \sim 20$  GeV should be weaker than those from other experiments [59–65]. On the other hand, below  $m_{N_R} \lesssim 4$  GeV there are already very strong limits on active-sterile mixing angles from other searches – lepton number violating meson decays, peak searches in meson decays, beam dump experiments and so on (Please see for instance [42] and references therein). Some of the planned experiments in this mass range, such as DUNE [94, 95] and SHiP [96, 97], are projected to have the capability to probe mixing angles all the way down to  $|\mathcal{U}_{\mu N}|^2 \sim 10^{-10}$ . We therefore sharpen

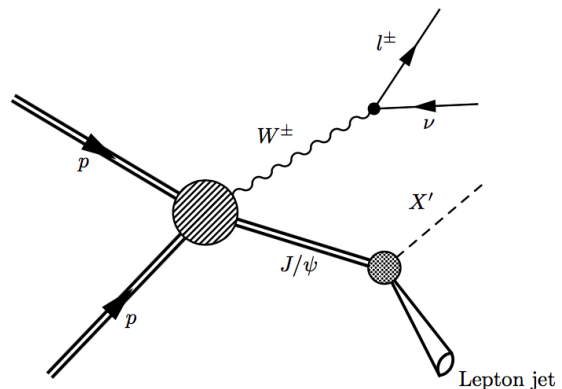


FIG. 3. A possible background from heavy flavor decays. Here, a  $J/\psi$  resonance is produced in association with a  $W^\pm$ . The decay products from the boosted  $J/\psi$  fake a lepton-jet while the  $W^\pm$  furnishes a prompt lepton. A relatively significant fraction of such events could still survive after a naive selection. They must therefore be accounted for more carefully while making an optimised analysis.

our mass-regime of interest to be between

$$4 \text{ GeV} < m_{N_R} < 25 \text{ GeV} . \quad (17)$$

In this mass regime of interest, for small sterile-active mixing  $|\mathcal{U}_{\mu N}|^2$ , one also expects from Eq. (16), the lepton-jet to be displaced appreciably from the primary vertex due to the large  $N_R$ -boost. This displacement may potentially be leveraged to discriminate between signal and background. Nevertheless, as we shall explain in Sec. IV this criterion turns out to be less significant, rather counterintuitively from naive reasoning, for overall signal sensitivity.

The presence of the prompt isolated lepton in the signal topology significantly simplifies the trigger needed for such a topology. Typical isolated lepton triggers at the ATLAS or CMS experiments have  $p_T$  thresholds ranging from 23 GeV for muons to 35 GeV for electrons. In addition, advanced trigger strategies such as those employed in Ref. [92] can also be constructed. At a hadron collider such as the LHC, a large source of single isolated prompt leptons is SM  $W^\pm$  production. Along with direct production,  $W^\pm$  also arise through the decay of  $t$ -quarks. The cross sections for  $t$ -quark production ( $t\bar{t}$  and single-top events) are also significant compared to signal at the LHC. Other standard model processes that give rise to more than one isolated prompt leptons are  $Z/\gamma^*$ , or  $WZ$  production,

can also lead to background to a final state with a prompt lepton.

Muons generally provide cleaner lepton and lepton-jet signals as compared to electrons or  $\tau$  leptons. Muons are reconstructed using the tracking chambers and therefore gives a better lepton-jet discriminant. For our conservative estimates we shall therefore assume that there is only appreciable mixing between a single sterile state and the muon-neutrino ( $\nu_\mu$ ). After analysis, this would therefore translate to a stricter limit on  $|\mathcal{U}_{\mu N}|^2$  as a function of the sterile neutrino mass  $m_{N_R}$ . If other channels are open then the limits obtained in a prompt-muon and muon-lepton-jet final state analysis will be weaker.

The requirement of a lepton-jet should significantly reduce the  $W^\pm$  and top backgrounds. But at hadron colliders,  $W^\pm$  are typically accompanied by light hadrons in a large fraction of events. Several light hadrons such as the  $J/\psi$  and the  $\Upsilon$  decay to a pair of oppositely-charged leptons. When these light hadrons are boosted, the resultant dilepton decay may mimic the lepton-jet of the signal (Fig. 3). This background can be reduced by raising the  $p_T$  thresholds on the lepton-jet muons and placing strict requirements on hadronic activity. However given that almost 6% of all  $J/\psi$ 's decay to a purely dimuon final state, such requirements will not remove this background completely.

The other significant background could come from  $t\bar{t}$  events. The  $t\bar{t}$  semi-leptonic decay chain results in one prompt lepton, two  $b$ -quarks, and two light quarks ( $t\bar{t} \rightarrow W^\pm b W^\mp \bar{b} \rightarrow \ell^\pm \nu q \bar{q}' b \bar{b}$ ). A potential decay chain for the  $b$ -hadrons is through semileptonic decay to  $c$ -hadrons which subsequently decay semileptonically to lighter particles. Such a decay chain can also give rise to two oppositely-charged leptons. Given the boost of the  $b$ -quark, these two leptons can mimic the signature of a lepton-jet. Thus both  $W$ -boson production, and  $t\bar{t}$  production can result in significant background to a prompt lepton + lepton-jet final state. An example of a final state that could arise from the  $t\bar{t}$  background is illustrated in Fig. 4. A requirement of low hadronic activity in the event will suppress the  $t\bar{t}$  background considerably, but not remove it completely. Further suppression can be obtained by requiring the lepton-jet to be isolated, i.e. by requiring low hadronic activity in the immediate neighbourhood of the lepton-jet.

Other small contributions arise from single-top production, as well as low rate processes such as  $Z \rightarrow 4\ell$ ,  $Z + b\bar{b}$ , or  $WZ/W\gamma^*$ . The  $Z \rightarrow 4\ell$  process where an asymmetric internal conversion takes place [98] can result in a soft muon appearing almost collinear to one of

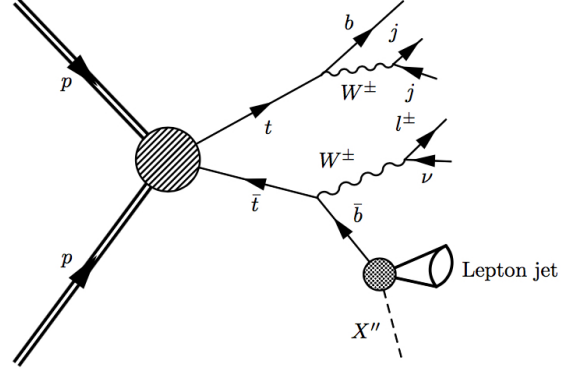


FIG. 4. A prototypical background topology that may arise from  $t\bar{t}$  events. Even vetoing for hadronic activity and imposing isolation requirements, potentially a large fraction of such events could contaminate the signal region.

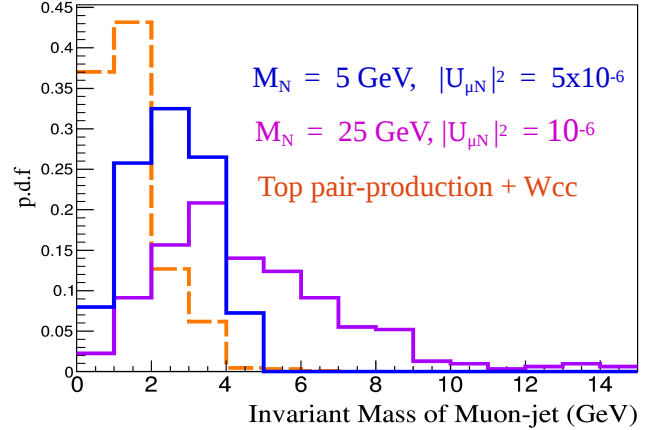


FIG. 5. The invariant mass of the  $\mu$ -Jet muons is shown for two signal points and for the combined background ( $t\bar{t}$  and  $W$ +jets) for a 13 TeV collider.

the muons from the  $Z$ -decay. This background as well as background from  $Z + b\bar{b}$  and  $WZ$  can be reduced to negligible levels by vetoing events that have more than one isolated lepton, and by requiring that the invariant mass of all three muons in the event is below the  $W$ -mass. The  $W\gamma^*$  background can be further reduced by considering the alignment of the missing energy with the  $\mu$ -Jet.

Fig. 5 shows the invariant mass constructed from the two muons that form the  $\mu$ -Jet. The signal distribu-

tion, as expected, peaks at harder values with increasing  $m_{N_R}$ . The background is concentrated at low values, since it arises primarily from  $b$ -hadron as well as lighter hadron decay. We do not use the invariant mass in our study as we find that it inordinately affects signal acceptance for low mass sterile neutrinos. We now proceed to detail the search strategy and discuss the prospective reach attainable at hadron colliders.

#### IV. LEPTON JET PROBES OF STERILE NEUTRINOS AT THE LHC AND FCC-hh/SppC

The signal mass-region of interest presents unique challenges and necessitates a careful analysis strategy, taking into consideration all the features of the signal and background topologies discussed in the previous section. Our aim is to carefully account for the relevant backgrounds and tailor the selection criteria to enable an optimal search strategy at a hadron machine. We will present our results in the context of the 13 TeV HL-LHC, and the proposed 100 TeV FCC-hh/SppC colliders [56, 57].

As mentioned, we will assume that there is appreciable mixing only between the sterile state and muon-neutrinos to set a conservative limit. This is partially motivated by the fact that at the LHC, muons will provide a cleaner lepton and lepton-jet signal as compared to electron or tau leptons. Identifying lepton-jets with electrons and taus require a more careful understanding of how hadronic objects might be wrongly reconstructed or misidentified as lepton-jets. Muons on the other hand are reconstructed using the tracking chambers and this gives a better measurement of the kinematics. With this consideration we will also take the prompt lepton and lepton-jet to be muonic.

In the  $4 \text{ GeV} < m_{N_R} < 25 \text{ GeV}$  mass-range, the dominant mode of production for  $N_R$  is via an on-shell  $W^\pm$  boson, as in Fig. 2. The  $N_R$  is produced in association with a prompt muon

$$W^\pm \rightarrow N_R + \mu^\pm.$$

The cross-sections for this production channel could differ by an order of magnitude between a 13 TeV and 100 TeV hadron collider. In Fig. 6 we illustrate this variation for the production cross-section in the case of  $m_{N_R} = 8 \text{ GeV}$ , as a function of the mixing. As we shall see, in the case of the backgrounds this increase can be even more drastic presenting challenges at 100 TeV.

After production, we will consider the fully leptonic decay of the  $N_R$ , proceeding via an off-shell  $W^{\pm*}$  or

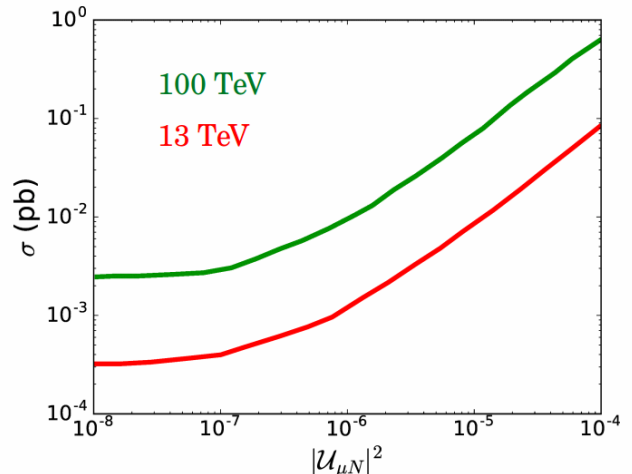


FIG. 6. The production cross section for a sterile, right-handed neutrino in association with a lepton, generated via on-shell  $W^\pm$  decay. The plot is for  $m_{N_R} = 8 \text{ GeV}$  and the variation is shown as a function of the mixing. The two curves are for the 13 TeV (red) and 100 TeV (green) cases.

$Z^{0*}$  boson

$$\begin{aligned} N_R &\rightarrow \mu^\mp + W^{\pm*} \rightarrow \mu^\mp + \mu^\pm + \nu_\mu \\ &\hookrightarrow \nu_\mu + Z^{0*} \rightarrow \nu_\mu + \mu^\mp + \mu^\pm. \end{aligned} \quad (18)$$

We optimize our analysis for the case where the  $N_R$  is boosted. This results in the final state muons and neutrino arising from its decay to be collimated. Thus our signal lepton-jet of specific interest is a muon-lepton-jet

$$\mu\text{-Jet} : \langle \mu^\pm \mu^\mp \nu_\mu \rangle$$

where the muons and neutrino are tightly collimated in a small cone-radius. We will require these pair of muons to be within a cone of radius  $\Delta R < 0.5$ , where  $\Delta R = \sqrt{\Delta\eta^2 + \Delta\phi^2}$ . We will refer to this object as a muon-jet or  $\mu$ -Jet henceforth.

Due to the boost of the  $N_R$  and small mixing angles, the  $\mu$ -Jet will be displaced from the prompt muon at the primary vertex. So, the characteristic signal being searched for consists of a prompt muon and a displaced  $\mu$ -Jet.

We generate the signal processes using MadGraph5\_aMC@NLO [99] for both 13 TeV and 100 TeV. The parton showering and hadronization are performed using Pythia 8.219 [100] with Tune 4C used to simulate the busy hadronic environment. The hadronized output is then passed through the



Delphes 3.3.2 [101] detector simulation. We use the default CMS and FCC detector cards for 13 TeV and 100 TeV respectively.

The dominant SM backgrounds arise from  $W^\pm$  production in association with jets and from  $t\bar{t}$  production. The  $Z \rightarrow 4\ell$  and  $WZ$  backgrounds are reduced by demanding the invariant mass of the  $\mu$ -Jet with the prompt muon,  $m_{\mu\text{-Jet-prompt}\mu} < 80$  GeV. The additional vetoing of a second prompt muon helps to completely remove the contribution from  $Z$ , and  $WZ$  processes. These selections do not impact the signal given the lack of a second prompt muon in the signal, and since the signal process begins with an on-shell  $W$  boson.

The background processes also follow the same simulation chain as the signal. The exact efficiencies of reconstructing non-standard objects, such as muon-jets, at a future 100 TeV detector are of course less well understood, and must await a detailed description of the final detector design. We do our analysis using generator level hadronized output at both 13 TeV and 100 TeV. To assess the effect of reconstruction efficiency on the signal, we consider two scenarios: a per-muon efficiency of 90%, which will result in an event efficiency of about 70%, and a per-muon efficiency of 80%, which will result in an event efficiency of about 50%. We start by making a selection for the prompt muon. We require the prompt muon to satisfy  $p_T > 22$  GeV, and  $|\eta| < 2.4$ . We then also make additional requirements on the impact parameter of the muon to ensure promptness, while requiring the muon to be isolated. At the LHC, this prompt isolated muon can be used to trigger the event. For the  $\mu$ -Jet, we start with selections based on the unique kinematics and topology of the signal, and subsequently impose further criteria that help to discriminate against dominant backgrounds, that may still contaminate the signal region.

Overall, our signal selection criteria may be listed as:

- S0 : Require an isolated, prompt muon with  $p_T > 22$  GeV, and  $|\eta| < 2.4$ . Transverse impact parameter  $d_{XY} < 0.2\text{mm}$  and  $d_Z < 0.1\text{mm}$ . The prompt muon is required to have the relative isolation,  $\frac{\Sigma p_{\text{trk}}}{p_T} < 25\%$ . Here  $\Sigma p_{\text{trk}}$  is the sum of transverse momentum of all charged particles with  $p_{\text{trk}} > 1$  GeV around a cone of  $\Delta R < 0.4$  from the prompt muon.
- S1: We require the  $\mu$ -Jet to be composed of a pair of muons with opposite charge, and with

$p_T > 2$  GeV and  $|\eta| < 2.4$ . This pair of muons should also satisfy  $\Delta R < 0.5$ . The  $\mu$ -Jet 4-vector is constructed by adding the 4-vectors of the two muons which form the  $\mu$ -Jet.

- S2: We require the invariant mass of the  $\mu$ -Jet with the prompt muon,  $m_{\mu\text{-Jet-prompt}\mu} < 80$  GeV. We also require that there is not more than one prompt muon per event. Both these requirements reduce the contribution from  $Z \rightarrow 4\ell$  to negligible levels. In addition since the signal is produced starting with an on-shell  $W$ -boson, we also expect the invariant mass to not contribute beyond the  $W$ -boson mass.
- S3: The signal does not have significant hadronic activity, while the primary backgrounds have jets. We require  $H_T < 60$  GeV, where  $H_T$  is defined as the scalar sum of  $p_T$  of all AK4 jets in the event with  $p_T > 30$  GeV. This selection reduces both the  $t\bar{t}$  and the  $W^\pm$ +Jets background.
- S4: The azimuthal angle between the missing transverse energy (MET) and the  $\mu$ -Jet should satisfy  $\Delta\phi_{\text{muon-jet-MET}} < 0.5$ . This selection suppresses the  $t\bar{t}$  background and the  $W^\pm$ +Jets background, where the  $\Delta\phi_{\text{muon-jet-MET}}$  has no preferential value.
- S5: We construct an isolation variable for the  $\mu$ -Jet as the sum of transverse momenta of all charged tracks with  $p_T > 1$  GeV within a cone of  $\Delta R < 0.6$  from the  $\mu$ -Jet. We require this sum to be less than 3 GeV. This selection strongly discriminates against the  $t\bar{t}$  and  $W^\pm$ +Jets background since the muons in these processes are accompanied by hadronic activity.

At 100 TeV, the fraction of signal events that are produced in the forward direction increases as compared to 13 TeV. The existing LHC experiments have coverage up to  $|\eta| < 2.5$  for muons, and  $|\eta| < 5$  for the calorimeters. We have considered that the detectors at a future 100 TeV collider will have extended muon coverage, as compared to present detectors, and thus we modify our selection to  $|\eta| < 5.0$  for all muons in our 100 TeV analysis. But being in the narrow  $4 \text{ GeV} < m_{N_R} < 25 \text{ GeV}$  signal regime, we find that most kinematic quantities of interest, such as the  $p_T$  of muons, MET etc. are quite similar between 13 TeV and 100 TeV. We have therefore adopted, as evident from selection criteria S0-S5 earlier, identical selections for 13 TeV and 100 TeV studies. We have performed

cross-checks to ensure the robustness of these assumptions.

In Fig. 7(a) we show the azimuthal angle between the missing transverse energy (MET) and the  $\mu$ -Jet for signal and the combined background ( $t\bar{t}$  and  $W$ +jets) for a 13 TeV collider. As expected the signal is concentrated at the lower end, while the background has a uniformly distributed value of  $\Delta\phi_{\text{muon-jet-MET}}$  on average. Fig. 7(b) shows the isolation of the  $\mu$ -Jet of the signal and the combined background ( $t\bar{t}$  and  $W$ +jets) for the 13 TeV collider after our signal selections S0 through S2 have been imposed. The  $t\bar{t}$  production ( $t \rightarrow Wb \rightarrow \ell\nu b$ ) and the  $W$ +jets gives rise to muons in a cascade decay. Hence due to their busy hadronic environment, the  $\mu$ -Jet for the backgrounds are lesser isolated than the signal. We also consider cosmic-rays as a background. Given our topology a cosmic-ray can only act as a background if it passes through the interaction point (thus acting as the prompt muon in the event, and one of the  $\mu$ -Jet muons). Following the estimate presented in Ref. [55], we consider this background to be negligible.

Previous studies have considered the impact-parameter and displacement of the  $\mu$ -Jet muons to be a sharp discriminating variable, against background, and have made selections for displaced muon-jets. We find that placing too hard a cut on these variables actually reduces overall sensitivity to events where the  $\mu$ -Jet is sometimes less displaced. It is also found that after other selection criteria it does not impact the remaining dominant  $Wc\bar{c}$  or  $t\bar{t}$  backgrounds significantly. The primary backgrounds arising from  $t\bar{t}$  decay involve  $b$ -hadrons. These  $b$ -hadrons have lifetimes of order  $c\tau \sim 500\mu\text{m}$ , resulting in muon displacement distributions that appear similar to signal over a significant part of the parameter space. Given these reasons, we do not actually make any hard impact-parameter requirements or displacement requirements for the  $\mu$ -Jet muons.

Given the selections described above (S0 through S5), Table I shows the acceptance for signal and background for our 13 TeV analysis, while Table II shows the same for the 100 TeV analysis. It is evident that the veto on hadronic activity, and the  $\Delta\phi$  requirement between the  $\mu$ -Jet and MET reduces the background drastically while maintaining high signal sensitivity. As an alternative to the hadronic activity veto, as a cross-check, we also performed a separate study using  $b$ -tagging to assess the impact on the  $t\bar{t}$  background. For this study, we considered the  $b$ -tagging efficiency from the CMS experiment [102]. We find, perhaps unsurprisingly, that an overall hadronic activity veto

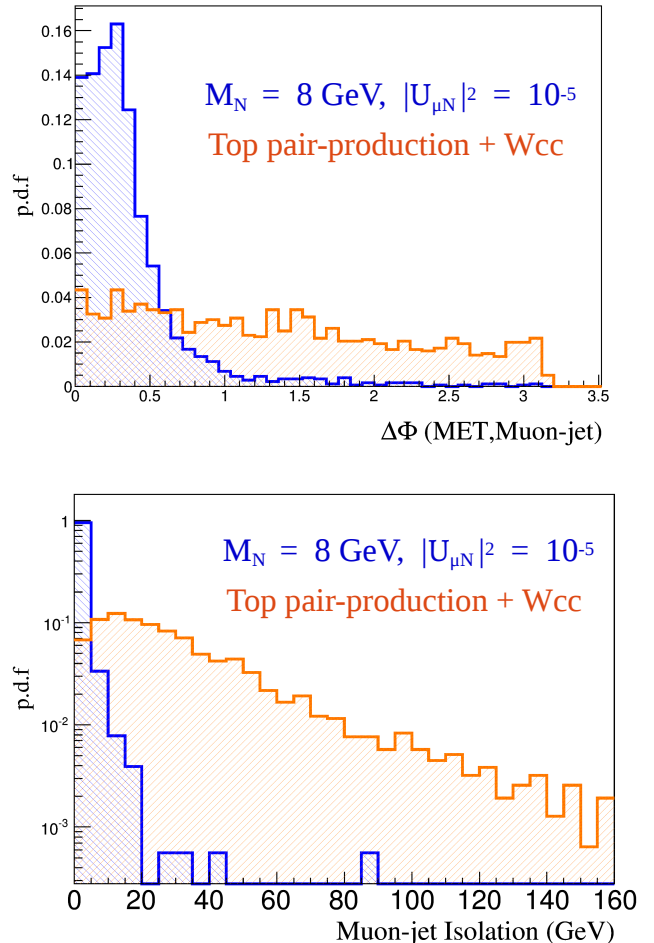


FIG. 7. Depicted on top is the azimuthal angle between the missing transverse energy (MET) and the  $\mu$ -Jet for signal and the combined background ( $t\bar{t}$  and  $W$ +jets) for a 13 TeV collider. As expected the  $\Delta\phi_{\text{muon-jet-MET}}$  peaks at a lower value for the signal while showing no particular preference for any value for the backgrounds. Shown on the bottom is the isolation of the  $\mu$ -Jet for the signal and combined background. The  $\mu$ -Jet for the backgrounds is much lesser isolated due to busy hadronic activity. Both of these are obtained after the selections S0 through S2 have been imposed.

acts as a better background discriminant than using  $b$ -tags given the typical  $b$ -tagging efficiencies of 90% with misidentification rate of about 1%.

In Fig. 8, we compare the final estimated sensitivity for our selections. Existing constraints are shown as dotted curves. The contours are for 13 TeV LHC with  $300 \text{ fb}^{-1}$  data (red) and 100 TeV FCC-hh/SppC

TABLE I. The acceptance for signal and background for the 13 TeV analysis.

Selections	Signal	$t\bar{t}$	Wcc
S0:Acceptance [%]	47.8	22.6	67.3
S1:Acceptance [%]	18.9	$3.5 \times 10^{-1}$	$2.1 \times 10^{-2}$
S2:Acceptance [%]	17.9	$2.6 \times 10^{-1}$	$1.6 \times 10^{-2}$
S3:Acceptance [%]	16.6	$6.7 \times 10^{-4}$	$10^{-2}$
S4:Acceptance [%]	13.4	$6.7 \times 10^{-4}$	$10^{-3}$
S5:Acceptance [%]	12.2	$5 \times 10^{-6}$	$2.3 \times 10^{-4}$

TABLE II. The acceptance for signal and background for the 100 TeV analysis.

Selections	Signal	$t\bar{t}$	Wcc
S0:Acceptance [%]	64.3	30.6	85.1
S1:Acceptance [%]	16.0	$4.1 \times 10^{-1}$	$3.2 \times 10^{-2}$
S2:Acceptance [%]	11.9	$2.5 \times 10^{-1}$	$2.5 \times 10^{-2}$
S3:Acceptance [%]	9.2	$7.4 \times 10^{-3}$	$6 \times 10^{-3}$
S4:Acceptance [%]	7.2	$3 \times 10^{-4}$	$2 \times 10^{-3}$
S5:Acceptance [%]	6.8	$3.5 \times 10^{-5}$	$3.1 \times 10^{-4}$

also assuming 300 fb<sup>-1</sup> data (green). We show 95% CL limits on  $|\mathcal{U}_{\mu N}|^2$  as a function of right-handed neutrino masses  $m_{N_R}$ . The limits were computed using the asymptotic limit method [103]-[106]. Assuming a 100% event reconstruction efficiency for signal, the upper limit on the signal cross-section is calculated to be  $\sigma_{\text{LIM}} = 9.03 \times 10^{-4}$  pb. If we consider efficiencies of 70% and 50%, the upper limit worsens to  $1.3 \times 10^{-3}$  pb and  $1.8 \times 10^{-3}$  pb respectively. As expected, the reach of the experiment will depend on the efficiency with which muons (and the signal events) are reconstructed. Note that at higher  $m_{N_R}$ , the sensitivity decreases since the daughter muons no longer satisfy the geometric criteria for a  $\mu$ -Jet. A high sensitivity at low  $m_{N_R}$  is maintained due to the extreme low momenta muons considered here.

As shown in Fig. 8, the 13 TeV LHC search optimised for this mass-regime is already competitive in sensitivity, if not slightly better in some regions, to the sensitivity of the proposed 100 TeV hadron collider. This may seem surprising and contrary to naive expectations. The primary reason is again the narrow [4 GeV, 25 GeV] signal region that we are trying to optimize over and the presence of strongly produced backgrounds that disproportionately increase when one moves from 13 TeV to 100 TeV. Even though

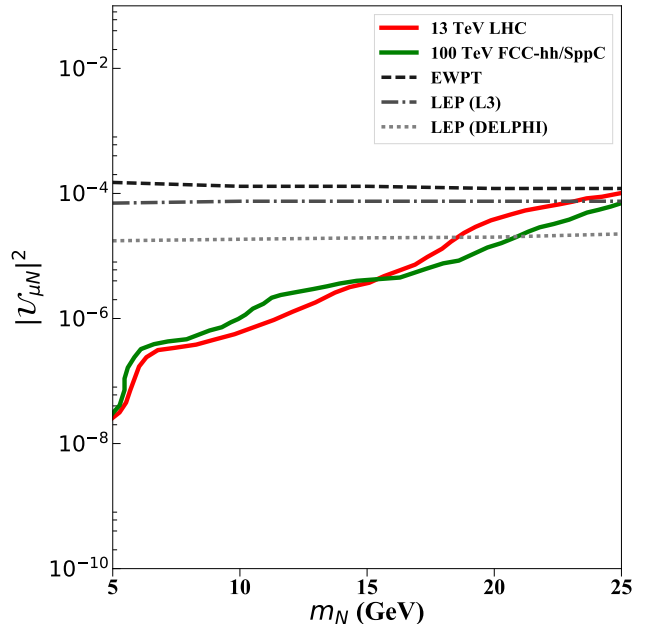


FIG. 8. Exclusion contours for the 13 TeV LHC (red) and the proposed 100 TeV FCC-hh/SppC (green), for similar selection criteria, assuming a signal efficiency of 100%. For the same integrated luminosity of 300fb<sup>-1</sup>, and for a similar cut based analysis, the LHC is already competent with a 100 TeV collider. Constraints from electroweak precision data (EWPT) [59–63] and LEP data (L3 and DELPHI collaborations) [64, 65] are also shown for comparisons.

the signal cross-section of our signal increases by an order of magnitude at the 100 TeV collider, as evidenced by Fig. 6, we observe that the background cross-section increases even more drastically – about 5 times as rapidly as the signal. This is of course expected as backgrounds like top-pair production feed off the strong production modes while our signal is dominantly produced solely via the weak interaction, in this regime. The drastic increase in background cross-sections at 100 TeV renders some of the signal cross-section increase and selection optimisations impotent. Thus, if our analysis and understanding is correct, for a 100 TeV hadron collider to do significantly better than the LHC, an increased detector coverage and algorithmic improvements, such as in b-tagging, might be required, along with more sophisticated search strategies. Based on our study, our current conclusion is therefore that the 13 TeV LHC, for the final states of interest, can give competitive limits in the [4 GeV, 25 GeV] sterile neutrino mass-regime.

## V. SUMMARY AND CONCLUSIONS

Sterile neutrino states are well motivated in many extensions of the Standard Model and have the potential to cast light on many unsolved questions in our theoretical frameworks. With the realization that their masses are not *a priori* fixed to any particular mass-scale, it becomes crucial to have search strategies spanning all the possible values.

We focused on a relatively unexplored mass regime ( $\Lambda_{\text{QCD}} \ll m_{N_R} \ll m_{W^\pm}$ ), where current constraints and experimental searches at hadron colliders are lacking. Also, prior theoretical studies in this signal region seem to have missed certain subtle, albeit crucial aspects of backgrounds and selection, while making sensitivity projections.

Motivated by the previous studies, unique signal topology and challenges singular to hadron colliders, we specifically revisited the sterile neutrino signal topology consisting of a prompt lepton and a displaced lepton-jet. We have attempted to make the first systematic study in this signal region, for the 13 TeV high-luminosity Large Hadron Collider and a future FCC-hh/SppC 100 TeV *pp*-collider.

For the same set of selection cuts, albeit for selection criteria optimised to each collider, our conclusion is that the 13 TeV HL- LHC may already be competitive with a future hadron collider. This is partially due to the fact that we are optimizing over a narrow mass-region in the low, electroweak regime for the signal – so the gains in signal cross-section while going to a higher energy machine are moderate – while the relevant backgrounds for the topology under consideration increase much more drastically. A higher de-

tector coverage, algorithmic improvements and a more sophisticated search strategy, in contrast to the simple cut and count based analysis we have performed, may possibly improve the reach at a 100 TeV *pp*-collider significantly. On the other hand a future  $e^+e^-$  collider may be able to significantly extend the sensitivities to very low mixing angles (see for instance [44] and references therein). Also, during the completion of this work an interesting study [107] appeared that looks for sterile neutrinos by reinterpreting displaced vertex searches ( $\mu jj$  final states) for long-lived particles at LHCb, during run-1 [108]. The study recasts current data and makes projections for future LHCb searches and the final limits are comparable to our study in the mass regime of interest; nevertheless with a different exclusion-limit functional profile.

A systematic and continuing program of sterile neutrino searches at current and future colliders, in all relevant mass ranges and topologies, would help in elucidating the nature of these states, if they exist, and help towards a complete coverage of interesting signal regions.

## ACKNOWLEDGEMENTS

We would like to thank S. Chauhan, E. Izaguirre, B. Shuve, S. Somalwar and S. Thomas for discussions and comments on the manuscript. S.D. and D.G are grateful to E. Izaguirre and B. Shuve for providing model files from their earlier study for corroboration and to S. Chauhan for help with simulation. The computations for the study were performed at the High Power Computing facility of the EHEP group at IISER, Pune.

- 
- [1] S. Chatrchyan *et al.* [CMS Collaboration], “Observation of a new boson at a mass of 125 GeV with the CMS experiment at the LHC,” Phys. Lett. B **716**, 30 (2012) [arXiv:1207.7235 [hep-ex]].
  - [2] G. Aad *et al.* [ATLAS Collaboration], “Observation of a new particle in the search for the Standard Model Higgs boson with the ATLAS detector at the LHC,” Phys. Lett. B **716**, 1 (2012) [arXiv:1207.7214 [hep-ex]].
  - [3] D. McKeen, J. L. Rosner and A. M. Thalapillil, Phys. Rev. D **76** (2007) 073014 doi:10.1103/PhysRevD.76.073014 [hep-ph/0703177].
  - [4] A. Aguilar *et al.* [LSND Collaboration], Phys. Rev. **D64**, 112007 (2001). [hep-ex/0104049].
  - [5] A. A. Aguilar-Arevalo *et al.* [ The MiniBooNE Collaboration ], Phys. Rev. Lett. **105**, 181801 (2010). [arXiv:1007.1150 [hep-ex]]
  - [6] E. Zimmerman [ MiniBooNE Collaboration ], PANIC 2011; Z. Djurcic [ MiniBooNE Collaboration ] NUFAC 2011; E. D. Zimmerman [ MiniBooNE Collaboration ], [arXiv:1111.1375 [hep-ex]].
  - [7] G. Mention, M. Fechner, T. Lasserre, T. A. Mueller, D. Lhuillier, M. Cribier, A. Letourneau, Phys. Rev. **D83**, 073006 (2011). [arXiv:1101.2755 [hep-ex]].
  - [8] A. Donini and D. Meloni, Eur. Phys. J. C **22**, 179 (2001) [hep-ph/0105089].

- [9] M. Sorel, J. M. Conrad, M. Shaevitz, Phys. Rev. **D70**, 073004 (2004). [hep-ph/0305255].
- [10] A. Dighe and S. Ray, Phys. Rev. D **76**, 113001 (2007) [arXiv:0709.0383 [hep-ph]].
- [11] A. Donini, M. Maltoni, D. Meloni, P. Migliozzi and F. Terranova, JHEP **0712**, 013 (2007) [arXiv:0704.0388 [hep-ph]].
- [12] M. Maltoni and T. Schwetz, Phys. Rev. D **76**, 093005 (2007) doi:10.1103/PhysRevD.76.093005 [arXiv:0705.0107 [hep-ph]].
- [13] A. Donini, K. -i. Fuki, J. Lopez-Pavon, D. Meloni and O. Yasuda, JHEP **0908**, 041 (2009) [arXiv:0812.3703 [hep-ph]].
- [14] A. de Gouvea and T. Wytock, Phys. Rev. D **79**, 073005 (2009) doi:10.1103/PhysRevD.79.073005 [arXiv:0809.5076 [hep-ph]].
- [15] D. Meloni, J. Tang and W. Winter, Phys. Rev. D **82**, 093008 (2010) [arXiv:1007.2419 [hep-ph]].
- [16] A. E. Nelson, Phys. Rev. D **84**, 053001 (2011) [arXiv:1010.3970 [hep-ph]].
- [17] J. Kopp, M. Maltoni and T. Schwetz, Phys. Rev. Lett. **107**, 091801 (2011) doi:10.1103/PhysRevLett.107.091801 [arXiv:1103.4570 [hep-ph]].
- [18] G. Karagiorgi, arXiv:1110.3735 [hep-ph].
- [19] B. Bhattacharya, A. M. Thalapillil and C. E. M. Wagner, Phys. Rev. D **85**, 073004 (2012) doi:10.1103/PhysRevD.85.073004 [arXiv:1111.4225 [hep-ph]].
- [20] C. Giunti and M. Laveder, Phys. Rev. D **84**, 073008 (2011) doi:10.1103/PhysRevD.84.073008 [arXiv:1107.1452 [hep-ph]].
- [21] C. Giunti, [arXiv:1106.4479 [hep-ph]]; C. Giunti, M. Laveder, [arXiv:1107.1452 [hep-ph]].
- [22] V. Barger, Y. Gao, D. Marfatia, [arXiv:1109.5748 [hep-ph]].
- [23] F. P. An *et al.* [Daya Bay Collaboration], [arXiv:1704.01082 [hep-ex]].
- [24] P. Minkowski, Phys. Lett. B **67**, 421 (1977); M. Gell-Mann, P. Ramond and R. Slansky, *Supergravity*, North Holland, Amsterdam, 315 (1980); T. Yanagida, in *Proceedings of the Workshop on the Unified Theory and the Baryon Number in the Universe*, KEK, Tsukuba, Japan, 95 (1979); S. L. Glashow, in *Proceedings of the 1979 Cargese Summer Institute on Quarks and Leptons*, Plenum Press, New York, 687 (1980); R. N. Mohapatra and G. Senjanovic, Phys. Rev. Lett. **44**, 912 (1980); J. Schechter and J. W. F. Valle, Phys. Rev. D **22**, 2227 (1980); J. Schechter and J. W. F. Valle, Phys. Rev. D **25**, 774 (1982).
- [25] R. N. Mohapatra and J. C. Pati, Phys.Rev. **D11**, 566 (1975).
- [26] R. N. Mohapatra and J. C. Pati, Phys.Rev. **D11**, 2558 (1975).
- [27] G. Senjanovic and R. N. Mohapatra, Phys.Rev. **D12**, 1502 (1975).
- [28] E. Witten, Phys. Lett. **91B** (1980) 81. doi:10.1016/0370-2693(80)90666-8
- [29] S. Nandi and U. Sarkar, Phys.Rev.Lett. **56**, 564 (1986).
- [30] R. N. Mohapatra and J. W. F. Valle, Phys. Rev. **D34**, 1642 (1986).
- [31] R. N. Mohapatra, Phys. Rev. Lett. **56**, 561 (1986).
- [32] K. S. Babu and R. N. Mohapatra, Phys.Rev.Lett. **70**, 2845 (1993), hep-ph/9209215.
- [33] B. Bajc and G. Senjanovic, JHEP **08**, 014 (2007), hep-ph/0612029.
- [34] T. Asaka, S. Blanchet and M. Shaposhnikov, Phys. Lett. B **631** (2005) 151 doi:10.1016/j.physletb.2005.09.070 [hep-ph/0503065].
- [35] T. Asaka and M. Shaposhnikov, Phys. Lett. B **620** (2005) 17 doi:10.1016/j.physletb.2005.06.020 [hep-ph/0505013].
- [36] L. Canetti, M. Drewes and M. Shaposhnikov, Phys. Rev. Lett. **110** (2013) no.6, 061801 doi:10.1103/PhysRevLett.110.061801 [arXiv:1204.3902 [hep-ph]].
- [37] L. Canetti, M. Drewes, T. Frossard and M. Shaposhnikov, Phys. Rev. D **87** (2013) 093006 doi:10.1103/PhysRevD.87.093006 [arXiv:1208.4607 [hep-ph]].
- [38] K. Fujikawa, Prog. Theor. Phys. **113** (2005) 1065 doi:10.1143/PTP.113.1065 [hep-ph/0407331].
- [39] A. de Gouvea, Phys. Rev. D **72** (2005) 033005 doi:10.1103/PhysRevD.72.033005 [hep-ph/0501039].
- [40] F. del Aguila, J. A. Aguilar-Saavedra and R. Pittau, J. Phys. Conf. Ser. **53**, 506 (2006) doi:10.1088/1742-6596/53/1/032 [hep-ph/0606198].
- [41] A. Atre, T. Han, S. Pascoli and B. Zhang, JHEP **0905** (2009) 030 doi:10.1088/1126-6708/2009/05/030 [arXiv:0901.3589 [hep-ph]].
- [42] F. F. Deppisch, P. S. Bhupal Dev and A. Pilaftsis, New J. Phys. **17**, no. 7, 075019 (2015) doi:10.1088/1367-2630/17/7/075019 [arXiv:1502.06541 [hep-ph]].
- [43] P. S. B. Dev, PoS ICHEP **2016**, 487 (2016) [arXiv:1612.08209 [hep-ph]].
- [44] S. Antusch, E. Cazzato and O. Fischer, arXiv:1612.02728 [hep-ph].
- [45] S. Antusch, E. Cazzato and O. Fischer, JHEP **1612**, 007 (2016) doi:10.1007/JHEP12(2016)007 [arXiv:1604.02420 [hep-ph]].
- [46] J. C. Helo, M. Hirsch and S. Kovalenko, Phys. Rev. D **89**, 073005 (2014) Erratum: [Phys. Rev. D **93**, no. 9, 099902 (2016)] doi:10.1103/PhysRevD.89.073005, 10.1103/PhysRevD.93.099902 [arXiv:1312.2900 [hep-ph]].



- [47] C. O. Dib and C. S. Kim, Phys. Rev. D **92** (2015) no.9, 093009 doi:10.1103/PhysRevD.92.093009 [arXiv:1509.05981 [hep-ph]].
- [48] M. Mitra, R. Ruiz, D. J. Scott and M. Spannowsky, Phys. Rev. D **94**, no. 9, 095016 (2016) doi:10.1103/PhysRevD.94.095016 [arXiv:1607.03504 [hep-ph]].
- [49] A. Das, P. S. B. Dev and C. S. Kim, arXiv:1704.00880 [hep-ph].
- [50] A. Das, Y. Gao and T. Kamon, arXiv:1704.00881 [hep-ph].
- [51] V. Khachatryan *et al.* [CMS Collaboration], Phys. Lett. B **748**, 144 (2015) doi:10.1016/j.physletb.2015.06.070 [arXiv:1501.05566 [hep-ex]].
- [52] V. Khachatryan *et al.* [CMS Collaboration], JHEP **1604**, 169 (2016) doi:10.1007/JHEP04(2016)169 [arXiv:1603.02248 [hep-ex]].
- [53] G. Aad *et al.* [ATLAS Collaboration], JHEP **1507**, 162 (2015) doi:10.1007/JHEP07(2015)162 [arXiv:1506.06020 [hep-ex]].
- [54] A. M. Sirunyan *et al.* [CMS Collaboration], arXiv:1706.08578 [hep-ex].
- [55] E. Izaguirre and B. Shuve, Phys. Rev. D **91** (2015) no.9, 093010 doi:10.1103/PhysRevD.91.093010 [arXiv:1504.02470 [hep-ph]].
- [56] T. Golling *et al.*, [arXiv:1606.00947 [hep-ph]].
- [57] CEPC-SPPC Study Group, IHEP-CEPC-DR-2015-01, IHEP-TH-2015-01, IHEP-EP-2015-01.
- [58] G. Aad *et al.* [ATLAS Collaboration], JHEP **1411**, 088 (2014) doi:10.1007/JHEP11(2014)088 [arXiv:1409.0746 [hep-ex]].
- [59] F. del Aguila, J. de Blas, and M. Perez-Victoria, Phys.Rev. **D78**, 013010 (2008), 0803.4008.
- [60] E. Akhmedov, A. Kartavtsev, M. Lindner, L. Michaels, and J. Smirnov, JHEP **1305**, 081 (2013), 1302.1872.
- [61] L. Basso, O. Fischer, and J. J. van der Bij, Europhys.Lett. **105**, 11001 (2014), 1310.2057.
- [62] J. de Blas, EPJ Web Conf. **60**, 19008 (2013), 1307.6173.
- [63] S. Antusch and O. Fischer, (2015), 1502.05915.
- [64] L3 Collaboration, O. Adriani *et al.*, Phys.Lett. **B295**, 371 (1992).
- [65] DELPHI Collaboration, P. Abreu *et al.*, Z.Phys. **C74**, 57 (1997).
- [66] S. Shevchenko, CALT-68-1939.
- [67] C. Patrignani *et al.* [Particle Data Group], Chin. Phys. C **40** (2016) no.10, 100001. doi:10.1088/1674-1137/40/10/100001
- [68] V. N. Aseev *et al.* [Troitsk Collaboration], Phys. Rev. D **84**, 112003 (2011) doi:10.1103/PhysRevD.84.112003 [arXiv:1108.5034 [hep-ex]].
- [69] C. Kraus *et al.*, Eur. Phys. J. C **40**, 447 (2005) doi:10.1140/epjc/s2005-02139-7 [hep-ex/0412056].
- [70] B. A. Reid, L. Verde, R. Jimenez, O. Mena, JCAP **1001**, 003 (2010). [arXiv:0910.0008 [astro-ph.CO]].
- [71] M. C. Gonzalez-Garcia, M. Maltoni, J. Salvado, JHEP **1008**, 117 (2010). [arXiv:1006.3795 [hep-ph]].
- [72] P. A. R. Ade *et al.* [Planck Collaboration], Astron. Astrophys. **594**, A13 (2016) doi:10.1051/0004-6361/201525830 [arXiv:1502.01589 [astro-ph.CO]].
- [73] G. Drexlin *et al.*, Nucl. Phys. B (Proc. Suppl.) **145** (2005) 263-267
- [74] P. Langacker, Phys. Rept. **72**, 185 (1981). doi:10.1016/0370-1573(81)90059-4
- [75] J. C. Pati and A. Salam, Phys. Rev. D **10**, 275 (1974) Erratum: [Phys. Rev. D **11**, 703 (1975)]. doi:10.1103/PhysRevD.10.275, 10.1103/PhysRevD.11.703.2
- [76] D. Wyler and L. Wolfenstein, Nucl. Phys. B **218**, 205 (1983).
- [77] R. N. Mohapatra, Phys. Rev. Lett. **56** (1986) 561. doi:10.1103/PhysRevLett.56.561
- [78] R. N. Mohapatra and J. W. F. Valle, Phys. Rev. D **34**, 1642 (1986).
- [79] P. Langacker, Phys. Rev. D **58** (1998) 093017 doi:10.1103/PhysRevD.58.093017 [hep-ph/9805281].
- [80] Z. Chacko, L. J. Hall, T. Okui and S. J. Oliver, Phys. Rev. D **70** (2004) 085008 doi:10.1103/PhysRevD.70.085008 [hep-ph/0312267].
- [81] T. Gherghetta, Phys. Rev. Lett. **92** (2004) 161601 doi:10.1103/PhysRevLett.92.161601 [hep-ph/0312392].
- [82] M. Malinsky, J. C. Romao and J. W. F. Valle, Phys. Rev. Lett. **95**, 161801 (2005) [hep-ph/0506296].
- [83] M. Shaposhnikov, Nucl. Phys. B **763**, 49 (2007) [hep-ph/0605047].
- [84] A. de Gouvea, J. Jenkins and N. Vasudevan, Phys. Rev. D **75** (2007) 013003 doi:10.1103/PhysRevD.75.013003 [hep-ph/0608147].
- [85] J. Kersten and A. Y. Smirnov, Phys. Rev. D **76**, 073005 (2007) [arXiv:0705.3221 [hep-ph]].
- [86] M. B. Gavela, T. Hambye, D. Hernandez and P. Hernandez, JHEP **0909**, 038 (2009) [arXiv:0906.1461 [hep-ph]].
- [87] A. de Gouvea and W. C. Huang, Phys. Rev. D **85** (2012) 053006 doi:10.1103/PhysRevD.85.053006 [arXiv:1110.6122 [hep-ph]].
- [88] P. S. B. Dev, A. Pilaftsis and U. k. Yang, Phys. Rev. Lett. **112**, no. 8, 081801 (2014) doi:10.1103/PhysRevLett.112.081801 [arXiv:1308.2209 [hep-ph]].
- [89] J. C. Helo, S. Kovalenko and I. Schmidt, Nucl. Phys. B **853** (2011) 80 doi:10.1016/j.nuclphysb.2011.07.020 [arXiv:1005.1607 [hep-ph]].

- [90] CMS Collaboration [CMS Collaboration], CMS-PAS-EXO-17-006.
- [91] G. Aad *et al.* [ATLAS Collaboration], *JHEP* **1508**, 138 (2015) doi:10.1007/JHEP08(2015)138 [arXiv:1411.2921 [hep-ex]].
- [92] The ATLAS Collaboration, ATLAS-CONF-2016-042. ”
- [93] The CMS Collaboration, *Phys. Rev. D* **91** (2015) 052012 doi:10.1103/PhysRevD.91.052012 [arXiv:1411.6977 [hep-ex]].
- [94] R. Acciarri *et al.* [DUNE Collaboration], arXiv:1601.05471 [physics.ins-det].
- [95] R. Acciarri *et al.* [DUNE Collaboration], arXiv:1512.06148 [physics.ins-det].
- [96] S. Alekhin *et al.*, *Rept. Prog. Phys.* **79**, no. 12, 124201 (2016) doi:10.1088/0034-4885/79/12/124201 [arXiv:1504.04855 [hep-ph]].
- [97] G. De Lellis [SHiP Collaboration], *Nucl. Part. Phys. Proc.* **285-286**, 126. doi:10.1016/j.nuclphysbps.2017.03.023
- [98] R. C. Gray, C. Kilic, M. Park, S. Somalwar and S. Thomas, arXiv:1110.1368 [hep-ph].
- [99] J. Alwall *et al.*, *JHEP* **1407**, 079 (2014) doi:10.1007/JHEP07(2014)079 [arXiv:1405.0301 [hep-ph]].
- [100] T. Sjöstrand *et al.*, *Comput. Phys. Commun.* **191** (2015) 159 doi:10.1016/j.cpc.2015.01.024 [arXiv:1410.3012 [hep-ph]].
- [101] J. de Favereau *et al.* [DELPHES 3 Collaboration], *JHEP* **1402** (2014) 057 doi:10.1007/JHEP02(2014)057 [arXiv:1307.6346 [hep-ex]].
- [102] The CMS Collaboration, CMS-PAS-BTV-15-001 (2016)
- [103] T. Junk, *Nucl. Instrum. Meth. A* **434** (1999) 435 doi:10.1016/S0168-9002(99)00498-2 [hep-ex/9902006].
- [104] A. L. Read, Modified frequentist analysis of search results (the CLs method) in Workshop on Confidence Limits, Eds. F. James, L. Lyons, and Y. Perrin,. p. 81.
- [105] A L Read. Presentation of search results: the CL<sub>s</sub> technique. *J. Phys. G*, 28(10):2693–704, 2002.
- [106] Procedure for the LHC Higgs boson search combination in Summer 2011. Technical Report CMS-NOTE-2011-005. ATL-PHYS-PUB-2011-11, CERN, Geneva, Aug 2011.
- [107] S. Antusch, E. Cazzato and O. Fischer, arXiv:1706.05990 [hep-ph].
- [108] R. Aaij *et al.* [LHCb Collaboration], *Eur. Phys. J. C* **77**, no. 4, 224 (2017) doi:10.1140/epjc/s10052-017-4744-6 [arXiv:1612.00945 [hep-ex]].